WL-TR-92-2041

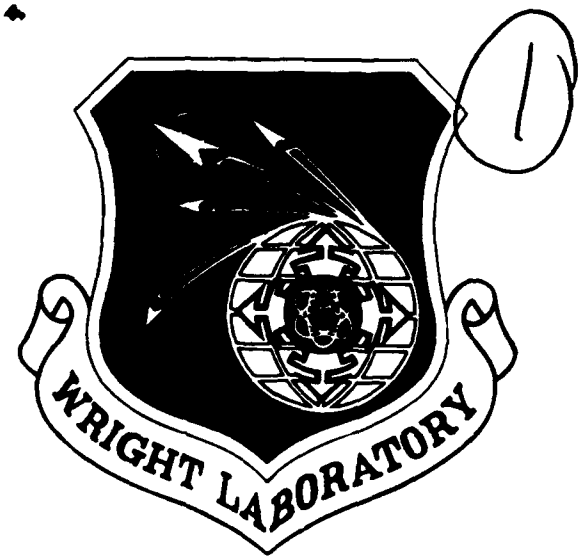

PHOTOVOLTAIC SYSTEMS BASED ON SPECTRALLY SELECTIVE HOLOGRAPHIC CONCENTRATORS

Jacques E. Ludman
Norhteast Photosciences
18 Flagg Road
Hollis, NH 03049

November 1991

Final Report for Period May 1991 to December 1991

AERO PROPULSION & POWER DIRECTORATE
WRIGHT LABORATORY
AIR FORCE MATERIEL COMMAND
WRIGHT PATTERSON AIR FORCE BASE, OHIO 45433-6563

NOTICE

When Government drawings, specifications, or other data are used for any purpose other than in connection with a definitely related Government procurement operation, the United States Government thereby incurs no responsibility nor any obligation whatsoever; and the fact that the Government may have formulated, furnished, or in any way supplied the said drawings, specifications, or other data, is not to be regarded by implication or otherwise as in any manner licensing the holder or any other person or corporation, or conveying any rights or permission to manufacture, use, or sell any patented invention that may in any way be related thereto.

This technical report has been reviewed and is approved for publication.

Steven F Adams
Project Engineer

James S. Cloyd
Acting Chief, Power Components Branch
Aero Propulsion & Power Directorate

FOR THE COMMANDER

MICHAEL D. BRAYDICH, Lt Col, USAF
Deputy Director
Aerospace Power Division
Aero Propulsion & Power Directorate

If your address has changed, if you wish to be removed from our mailing list, or if the addressee is no longer employed by your organization please notify WL/POOC, Wright-Patterson AFB OH 45433-6563 to help maintain a current mailing list.

Copies of this report should not be returned unless return is required by security considerations, contractual obligations, or notice on a specific document.

UNCLASSIFIED
SECURITY CLASSIFICATION OF THIS PAGE

REPORT DOCUMENTATION PAGE

Form Approved
OMB No. 0704-0188

1a. REPORT SECURITY CLASSIFICATION UNCLASSIFIED	1b. RESTRICTIVE MARKINGS NA
2a. SECURITY CLASSIFICATION AUTHORITY NA	3. DISTRIBUTION/AVAILABILITY OF REPORT UNLIMITED
2b. DECLASSIFICATION/DOWNGRADING SCHEDULE NA	
4. PERFORMING ORGANIZATION REPORT NUMBER(S) FY1455-91-08827 RPT-1	5. MONITORING ORGANIZATION REPORT NUMBER(S)
6a. NAME OF PERFORMING ORGANIZATION Northeast Photosciences 6b. OFFICE SYMBOL (If applicable) ---	7a. NAME OF MONITORING ORGANIZATION Wright Laboratory (WL/POOC-2)
6c. ADDRESS (City, State, and ZIP Code) 18 Flagg Road Hollis, NH 03049	7b. ADDRESS (City, State, and ZIP Code) Wright-Patterson AFB Ohio 45433-6563
8a. NAME OF FUNDING/SPONSORING ORGANIZATION Wright Lab 8b. OFFICE SYMBOL (If applicable)	9. PROCUREMENT INSTRUMENT IDENTIFICATION NUMBER F33615-91-C-2136
8c. ADDRESS (City, State, and ZIP Code) AERO SYSTEMS DIVISION USAP Wright-Patterson AFB Ohio 45433	10. SOURCE OF FUNDING NUMBERS PROGRAM ELEMENT NO. 63218C PROJECT NO. 1602 TASK NO. 04 WORK UNIT ACCESSION NO. 06

11. TITLE (Include Security Classification)
Photovoltaic Systems Based on Spectrally Selective Holographic Concentrators (UNCLASSIFIED)

12. PERSONAL AUTHOR(S)
Ludman, Jacques E.

13a. TYPE OF REPORT	13b. TIME COVERED	14. DATE OF REPORT (Year, Month, Day)	15. PAGE COUNT
Final	FROM 91-5-1 TO 91-12-1	91-11-28	55

16. SUPPLEMENTARY NOTATION
This is a Small Business Innovative Report, Phase I

17. COSATI CODES			18. SUBJECT TERMS (Continue on reverse if necessary and identify by block number)
FIELD	GROUP	SUB-GROUP	Solar, Holography, Spectrum Splitting

19. ABSTRACT (Continue on reverse if necessary and identify by block number)

(a) The purpose of the work was to demonstrate the feasibility of a new holographic technique for concentrating solar energy and splitting its spectrum with a single hologram to generate power, using two or more solar cells optimized at different portion of the solar spectrum.

(Continued on back page)

20. DISTRIBUTION/AVAILABILITY OF ABSTRACT	21. ABSTRACT SECURITY CLASSIFICATION
☒ UNCLASSIFIED/UNLIMITED ☐ SAME AS RPT. ☐ DTIC USERS	Unclassified
22a. NAME OF RESPONSIBLE INDIVIDUAL Steven Adams	22b. TELEPHONE (Include Area Code) 513-255-6235 22c. OFFICE SYMBOL WL/POOC-2

DD Form 1473, JUN 86 *Previous editions are obsolete.*

SECURITY CLASSIFICATION OF THIS PAGE
UNCLASSIFIED

(b) Various holographic materials, techniques for making holograms, and combinations of solar cells of different materials were investigated. Techniques were developed for testing system efficiencies. A number of potential problems and difficulties were successfully addressed. Holograms and solar cell systems were fabricated and tested, and demonstration units fabricated.

(c) Preliminary devices preformed as predicted. Holograms with efficiencies well above 90% were fabricated that were operable throughout the entire visible spectrum. Preliminary results demonstrated, as predicted, that relativity thin high-efficiency holograms would be required for this application. Holograms about twice the desired thickness (6 microns) were fabricated that showed very high efficiencies over the entire area of the holograms. These holograms did not have the extremely wide bandwidth desired, but they performed in accordance with theory. The technique for lying down appropriately thin films was advanced, and holograms were made with thin films (3 microns) that were reasonably uniform as well-behaved. Some regions of these holograms had very high efficiencies and the very broad widthbands (the solar spectrum) systems, such as silicon and gallium arsenide, is quite appropriate and will lead to an improvements of 90% over the conventional system cell with Fresnel concentrators and silicon solar cells.

(d) The use of holographic focusing and spectrum splitting together with multiple solar cells will provide greatly improved efficiency of power generation for space applications.

TABLE OF CONTENTS

INTRODUCTION

The problem being addressed is that of providing efficient photovoltaic power for space use by increasing the efficiency of conversion of solar radiation to electricity. This project has demonstrated a viable approach to this goal with a simple optical configuration based on spectrally dispersive holographic concentrators that are efficient, robust, and economical.

The innovative concept is a photovoltaic system based on spectrally selective holographic concentrators. Holography offers an ideal solution to the problems of solar concentration and spectrum splitting for photovoltaic conversion. The holographic elements themselves are light in weight, durable, and flat, and are thus highly suitable for deployment in a space environment. Solar holograms with efficiencies above 90% over the entire visible spectrum have already been demonstrated in a number of holographic materials, and some of these materials are inherently hard, showing resistance to damage from ultraviolet radiation and moisture. A proprietary holographic design is described here that in a single element focuses the incoming solar radiation at ratios 100:1 or better and also separates the spectral components. The design itself is shown in Fig 1. The hologram focuses the solar radiation into a narrow line in one dimension and spectrally disperses it in the other. The design of the system leads to a cell orientation that is at right angles to the hologram itself. The single hologram changes the direction of the incoming radiation, focuses it, and spectrally disperses it, in one operation. Since the hologram is a single

element, alignment is greatly simplified. The design represents a breakthrough and avoids the problems inherent in conventional holographic approaches that use combinations of lenses and filters, lenses and prisms, lenses and holograms, or tandem cells.

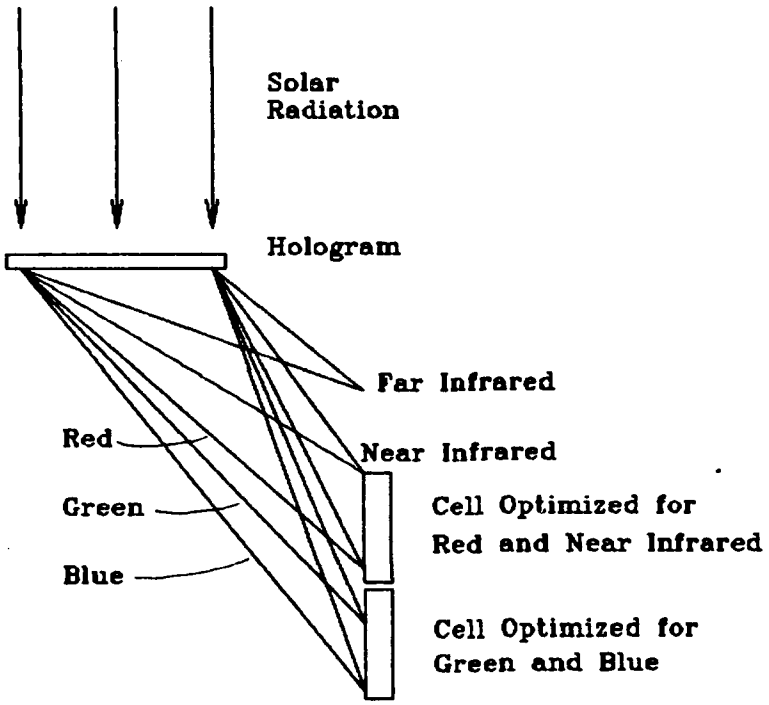

Fig 1. Holographic concentrator and spectrum splitter. One photocell is optimized for red and near infrared, the other for green and blue. Far infrared, which would contribute only useless heat, is diffracted away from the cells.

In the design of a photovoltaic system, a primary goal is to maximize the efficiency of the conversion of solar to electrical energy and thereby to minimize the losses. While some loss, perhaps as much as 15%, is inherent and stems from unavoidable causes, the mechanisms that are responsible for the highest losses by far are those which arise because the solar radiation is not monochromatic radiation with a wavelength that coincides

with the bandgap wavelength of a given photovoltaic cell. Thus there are losses because photons with wavelengths longer than the bandgap wavelength are not absorbed and are dissipated as heat, and there are losses because the energy in excess of the bandgap of short wavelength photons is all lost as heat. These two mechanisms alone account for about 55% of the losses in an airmass 1.0 (AM 1.0) concentration 100 spectrum in silicon. Because of these inherent losses the maximum theoretical efficiency for a silicon cell is only about 33%. Of course, the actual power conversion efficiencies are much lower, even in the laboratory. The highest conversion efficiency yet reported (for a GaAs cell, at 200 suns) is less than 24%.

In a standard solar cell work[1] the single- and two-cell experimental results, shown here in Table I, are described.

TABLE I

Cell Output Efficiencies for Various Systems

Cell(s)	Alone	As one of two cells	Improvement over Si	Improvement over GaAs
Si	15%	11%	--	--
GaAs	20%	18%	45%	--
Si--GaAs	29%	--	90%	45%
Si--AlGaAs	35%	--	133%	75%
Three-cell	40% (practical expectation)		167%	100%

Table I. Efficiencies of various materials as single cells and as elements of multi-cell systems. Note that adding the third cell provides improvement over a two-cell system using AlGaAs by only about 15%, a marginally worth-while gain.

Losses may be reduced considerably by using a combination of different cells to improve the match between photon energies and the bandgap energies. This is the basis of multijunction technology, based on either cascading or spectrum splitting. Multijunction cells tend to be complex and costly. Cascade cells must be carefully matched so that the current produced in each junction is the same; further, for concentrating systems, these cells must have good thermal conductivity to be able to dissipate the large amount of excess heat. Spectrum splitting can be based on dichroic mirrors. These are not highly efficient and have roll-off at the edges of their reflection curves; they also have Fresnel losses and introduce alignment problems.

This project has investigated the means of optimizing the direction and distribution of various energy bands onto photovoltaic cells matched to these energy bands. It has taken advantage of the new technology of holography to increase the efficiency of conversion of solar radiation into electricity. The holograms can be made robust, light weight, resistant to a space environment, and relatively economical. They can also diffract light with efficiencies close to 100% over most of the spectrum of interest. Relatively small cells will operate at very high efficiencies, and since long wavelength radiation is diffracted away, the heat dissipation requirements are minimized. This simple and elegant configuration relaxes the design constraints on the cells and allows an almost unlimited range of design and optimization possibilities.

HOLOGRAM FABRICATION

Principles

The principle behind the use of thick holograms for efficient collection, concentration, and dispersion of solar energy is the creation of a permanent pattern of variation in the index of refraction within a material. This pattern will diffract light in the desired manner with little or no absorption of the energy by the hologram itself. The pattern must exist through an appreciable thickness of the holographic material. The pattern is initially created by the interference of two mutually coherent laser beams. The interference pattern creates a pattern of regions that have different indices of refraction.

In dichromated gelatin, hexavalent chromium atoms are reduced to the trivalent state by blue-green light from an argon ion laser. The extent of the reduction is determined by the local intensity of the light, which varies with the phase of the interfering beams. In regions where the interference is constructive, the light intensity is high; where it is destructive, the intensity approaches zero. The trivalent chromium, in turn, causes the molecules of gelatin to cross-link, forming a rigid structure in those regions where the light intensity is high. After exposure, any remaining chromium is removed by soaking the gelatin in a sodium thiosulfate (hypo) solution to prevent further exposure to light from affecting the gel. The regions of greater cross-linking have a higher index of refraction.

Procedure

The procedure by which the holograms for this project were fabricated follows in general those reported by Saxby[2] and by McGrew[3]. The material is prepared by dissolving gelatin (a few percent by weight) in distilled water and then adding an appropriate amount of ammonium dichromate, which sensitizes it to blue-green light. The gel is liquefied by heating it to about 50° C, which gives it the right consistency for spreading. The material is spread upon the chosen substrate by laying a bead across the top of the substrate and rolling it into a uniformly thin film using a number 16 Mayer rod. It has been found that control of both the temperature at which the gel is spread and the humidity during the spreading process and afterward, while the gel is setting, is vital to the formation of a uniform layer. The humidity must be quite high (about 70%) to insure that the setting time is long enough to allow the material to relax into a thin uniform layer.

Uniformity of Thickness

It is important that the holographic coatings be relatively smooth. Uneven coatings can arise from imperfect cleaning and preparation of the substrate. Moderate unevenness is not important because the holographic pattern is self-adjusting to moderate variations in thickness. The thickness is important because of the relationship between the thickness of the film and the bandwidth of the diffracted radiation.

The efficiency η of a thick transmission phase hologram is given [4],[5],[6] by

$$\eta = \sin^2 (\pi n_1 d/\lambda \cos \theta) \qquad \text{Eq. (1)}$$

where n_1 is the index modulation and d is the thickness. The efficiency varies periodically, reaching 100% when the argument reaches odd multiples of $\pi/2$. For efficient holograms, Eq. (1) relates the thickness to the bandwidth.

Since the angular acceptance, or the angle to which the hologram may be tilted away from the normal to the incoming beam and still maintain substantial diffracted energy, is directly proportional to the bandwidth of the hologram and inversely proportional to its thickness, thin holograms have larger acceptance angles and broader bandwidths; very thick holograms must be very carefully aligned to the incoming radiation and will respond to only a very narrow bandwidth around the central wavelength.

The efficiency of the hologram may vary from point to point, owing to a number of causes:

(a) variations in intensity of either interfering beam

(b) variations in concentration of dichromate within the gel

(c) imperfections and distortions in the film due to non-uniform shrinkage during drying

(d) sensitivity of the gel to cross-linking

There are various coating technologies available, other than the one that we are using. The material may be spin-coated, spread with a knife edge, or sprayed, as well as being drawn with a Mayer rod.[2] Spin-coating controls the gel thickness very

well but is difficult to use over large areas. Spraying is easy to do, but the gel thickness is difficult to control, particularly for thin films.

The Mayer rod is a close-wound wire rod, which is used to distribute the gel evenly over the substrate by pulling the rod and gel across the substrate. Tnis technique controls the thickness and uniformity quite well, although there have been some problems when depositing thin layers. The process can easily coat surfaces as large as 10" X 12" using equipment that is commercially available. All techniques require controlled humidity and a dust-free drying room for optimum results.

Various factors may affect the uniformity of the film. If the humidity is too low, the gel may not only be non-uniform, but it may not be able to relax sufficiently, leading to a coating with an irregular surface. This is a problem with films drawn with a Mayer rod where the drawing surface is irregular to start. The chemistry of the material being laid down may also affect uniformity. A low gel-concentration film will take a little longer to dry because there is more liquid to evaporate but may have more time to relax. If the concentration of dichromate is too high, the dichromate may crystallize as it dries. The processing procedure is quite important and may use several different concentrations of alcohol successively. Too rapid removal of the water may distort the nearly parallel fringes into curves because of the more rapid removal near the hologram surface compared with that near the substrate. We are using two

alcohol concentrations, which appear to produce sufficiently uniform drying throughout the thickness of the film. The curing procedure, allowing the hologram to remain overnight, may be done at various humidities and temperatures. The optimum humidity, in our experiments, is between 70% and 80%. A variety of problems may occur during the curing process.(7)

There may well be a difference between the initial thickness of the gelatin and the final thickness of the hologram, due to shrinkage between the time of exposure and the time when the hologram has been developed, preserved, and protected. This has an effect on the peak transmission wavelength but, if the drying is uniform, only the peak wavelength and not the bandwidth will be affected. In the case of many of these holograms, the shrinkage is quite small and the peak wavelength shifts only slightly so that the optimum alignment for the hologram for 488nm is only slightly different from the normal. The small shift of The fabrication angle is shifted slightly, from 90° to 92°. This shift is small enough that demonstration packages and deliverables may be mounted normal to the beam without any noticeable effect. The peak wavelength shift is about 20 nm.

It should be noted that there is a major shift in angle if one is looking for peak intensity in the red. As noted in the section on hologram characterization, a hologram that is highly efficient at 488nm when mounted normal to the beam will be much less efficient for red wavelengths, such as 633nm, because of the geometry. If the hologram is tipped about ten degrees, the efficiency in the red can go up to 80% or 90%, while the

efficiency in the blue-green drops substantially. This is not a shrinkage effect, but a standard effect from the Bragg angle and efficiency equations.[6]

Setup

The setup for producing focusing dispersive holograms is shown in Fig 2. Two beams, beam B parallel and beam A diverging, traverse equal pathlengths and arrive coherently at the hologram to produce an interference pattern. The back surface of the substrate is coated with a light-absorbing material to prevent the Fresnel reflection from introducing unwanted fringe patterns of a reflection hologram. This layer is removed prior to processing. When the hologram is played back by impinging a collimated beam upon it (from the left, in this diagram), the interference pattern causes the beam to converge in the direction of the point from which the diverging beam came, producing a focused spot of light. The position of the spot, though, depends upon the wavelength. Light of the wavelength in which the hologram was made will focus to the apparent divergence point; other wavelengths, in accordance with the Bragg law, will be deflected at different angles.

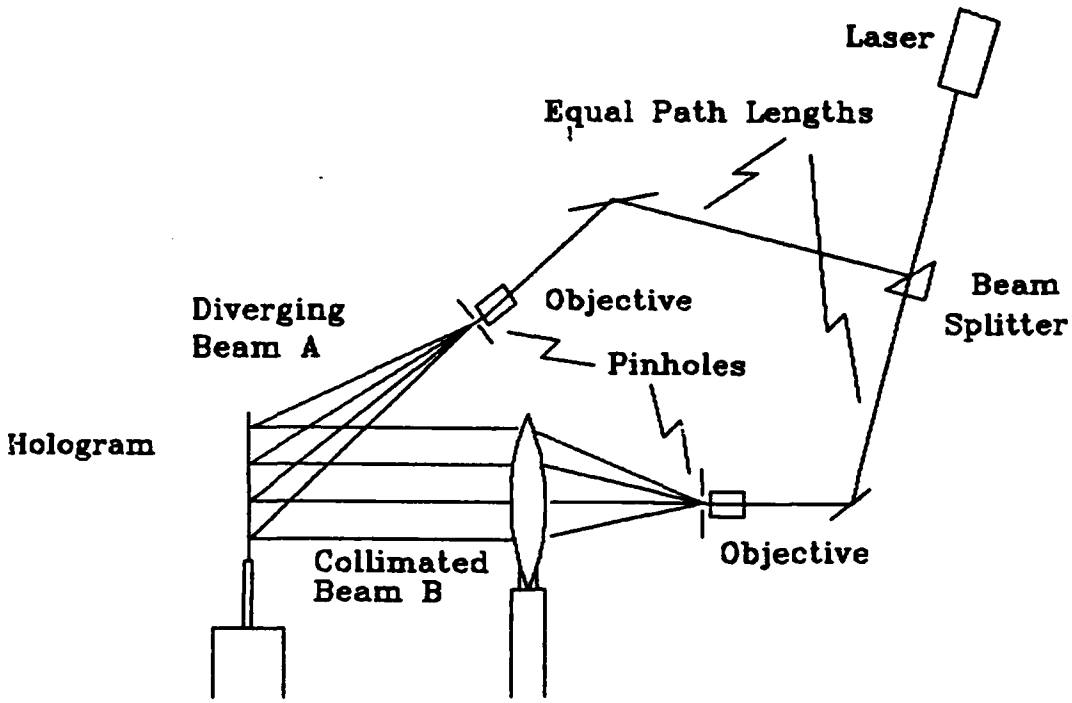

Fig 2. Setup for producing focusing dispersive holograms. Divergent beam A and parallel beam B are coherent, split by a beam splitter from a single laser beam and equal in path-length. Each beam goes through a microscope objective to diverge the beam and a pinhole to provide uniform intensity. Beam B is collimated to a parallel beam, while beam A remains divergent. In playback, the hologram is illuminated by sunlight coming from the opposite direction. The sunlight is diffracted by the hologram to retrace the path towards the focal point from which the divergent beam originated.

Uniformity of Beams

The sensitivity of the dichromated gelatin is 20 mj/cm^2 for a 10 μm thick hologram. With the setup we are using the output intensity is of the order of 600 mw, the power density of the combined interfering beams is of the order of 0.3 mw/cm^2, leading

therefore to exposure times on the order of 1 minute. If the interfering beams are not equal, the excess power in one beam does not affect the overall performance of the hologram, but simply provides a moderate background exposure, which leads to some cross-linking everywhere. The refractive index modulation occurs in those regions of the hologram where the two laser beams constructively and destructively interfere, and the length of exposure is calculated on the basis of the total intensity of the interfering beams. The excess of power in one beam over the other should be kept as small as possible to allow for maximum index variation.

Reflection from the Back Surface

Even a very small amount of reflection from the back surface of the holographic plate during exposure will lead to a spurious interference pattern that will reduce the overall efficiency. An antireflection coating of black spray paint is therefore applied to the back surface of the substrate prior to exposure and removed prior to fixing. The proper choice of absorbing paint can prevent reflection from occurring. The paint matches the refractive index of the substrate, and the pigment absorbs all transmitted radiation.

Fixing

After having been exposed for the required length of time, the hologram is fixed in quarter-hard hypo, washed in water and isopropyl alcohol baths of various concentrations to remove the residual water in the gelatin, and dried.[3] The exposure time

depends upon the intensity of the laser, the thickness of the film, and the chemical composition of the gel. Most of the holograms reported here were exposed for about 60 seconds.

Protection from Moisture

The holograms made from dichromated gelatin are quite susceptible to moisture unless steps are taken to protect them. High humidity or moisture will completely destroy the hologram, leaving a simple gel film. The protection process is as simple as coating the entire holographic surface with an optical glue and covering it with a cover plate of either a transparent plastic or glass. The stability of dichromated gelatin and other materials of potential use for this program are discussed in the section of this report on hardness of holographic materials.

HOLOGRAM CHARACTERIZATION

A hologram evaluation station was established at the University of Lowell to measure a number of characteristics of the holograms fabricated during the course of this Phase I research effort. This station is shown in Fig 3.

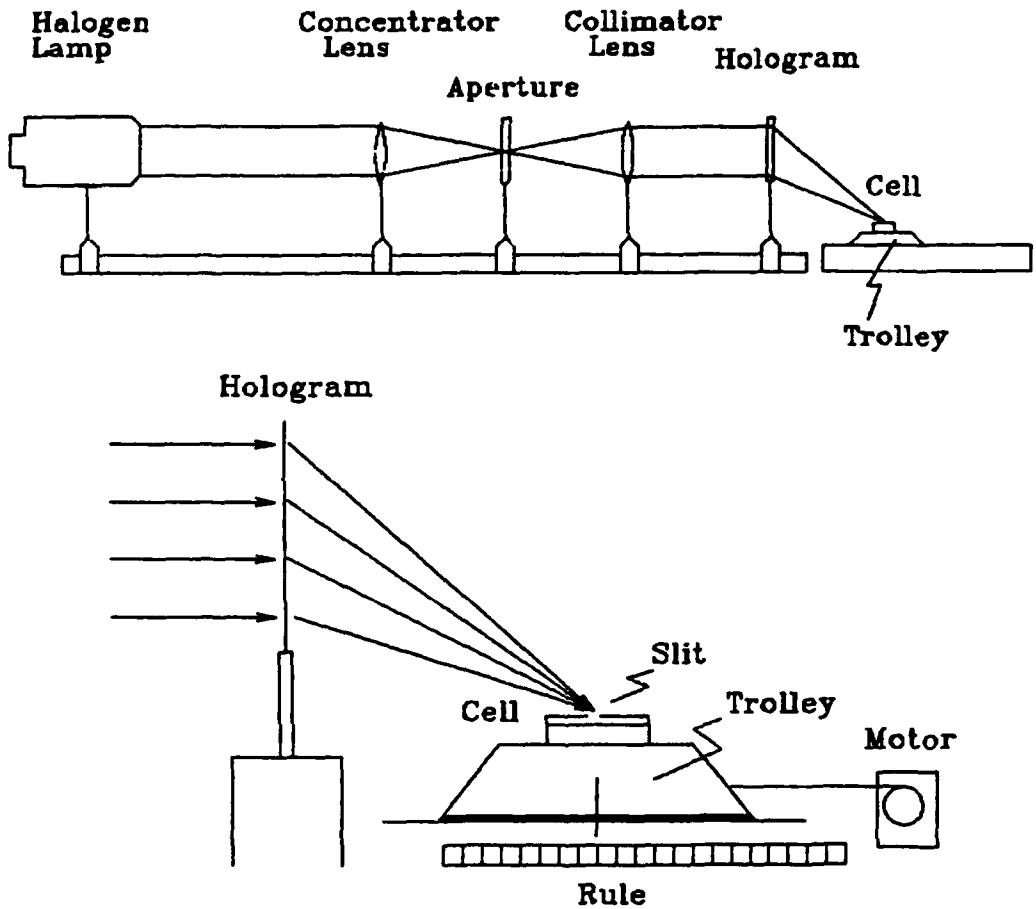

Fig 3. Light from a halogen lamp, focused through a collimating lens, impinges upon a hologram in a mount and is diffracted to a "rainbow line" on the surface of a solar cell masked with a slit 2 mm wide. The cell and slit are on a motor-driven assembly so that the entire spectral output of the hologram can be measured. A cosine correction must be made to the recorded output because the angle of the light arriving at the slit varies with the wavelength.

This station provides a substantial output over the entire spectral range of interest, and the silicon cell detector is appropriate for measuring all the wavelengths of interest. In particular, since the longest wavelength cell or choice is likely to be silicon itself, measurements of wavelengths beyond the bandgap of silicon are not necessary. The output of the halogen lamp, as characterized by the manufacturer, is shown in Graph 1. The output has some structure, and there is substantial power from 300nm to well beyond the wavelength cutoff of silicon at 1200nm. The output, originally in microwatts per lumen per nm is shown here in arbitrary units consistent with the holographic measurements in order to calculate accurately the efficiency (dimensionless) of the holograms.

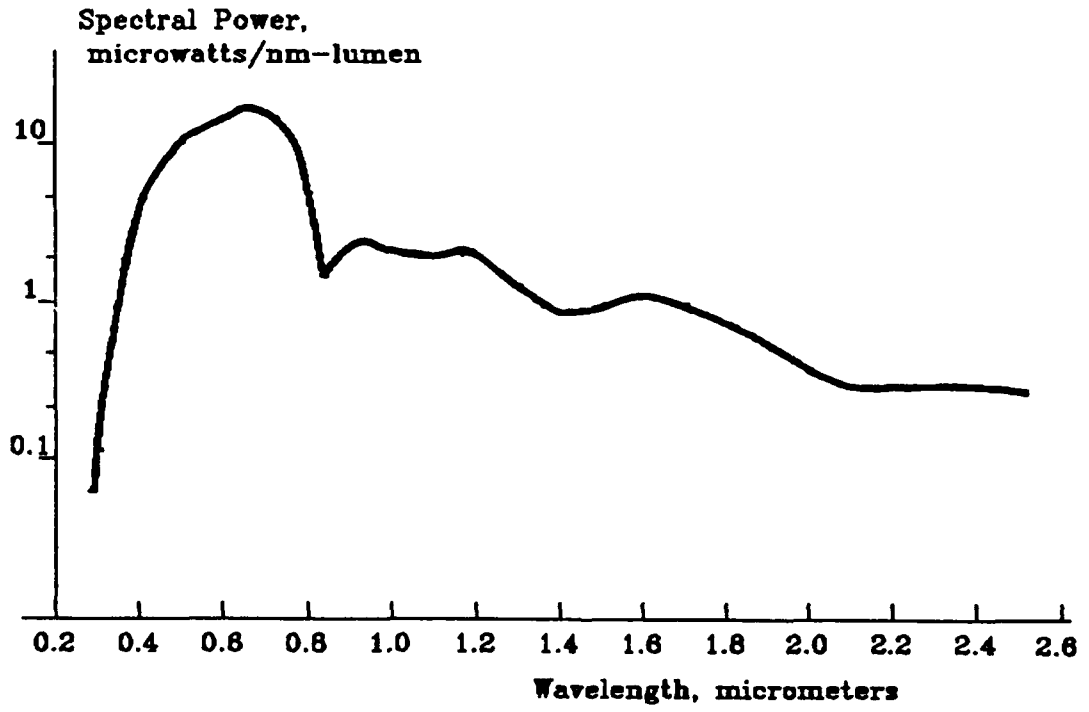

Graph 1. Output of the halogen lamp as a function of wavelength, as characterized by the manufacturer.

During the course of the work, two separate detector systems were used. One was a solar cell provided by Mobile Solar Corp., with an efficiency characterized by them as shown in Graph 2. The other was a conventional detector system. The curves from the two systems were very similar in shape. The solar cell itself was used for all characterizations of the holograms. The detector system was used solely to verify, with a prism, that the output power of the halogen source was indeed the output that was being measured by the solar cell.

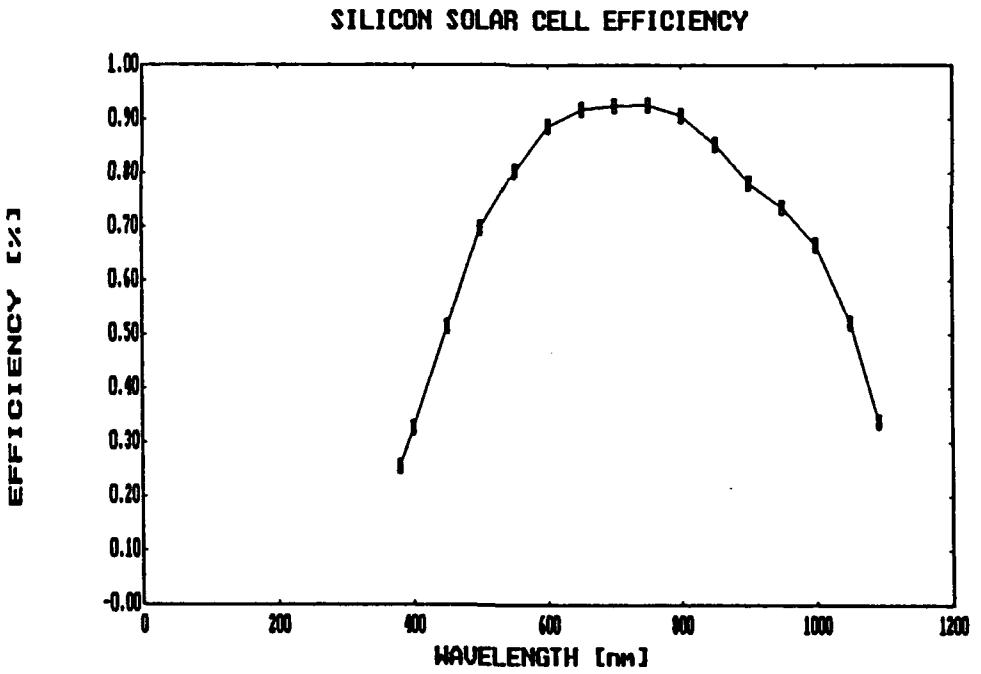

Graph 2. Efficiency of the solar cell as a function of wavelength, as characterized by the manufacturer.

Graphs 1 and 2 were multiplied together to yield the system performance, shown in Graph 3, since at each wavelength this

shows the current output of the cell for the corresponding output of the halogen lamp.

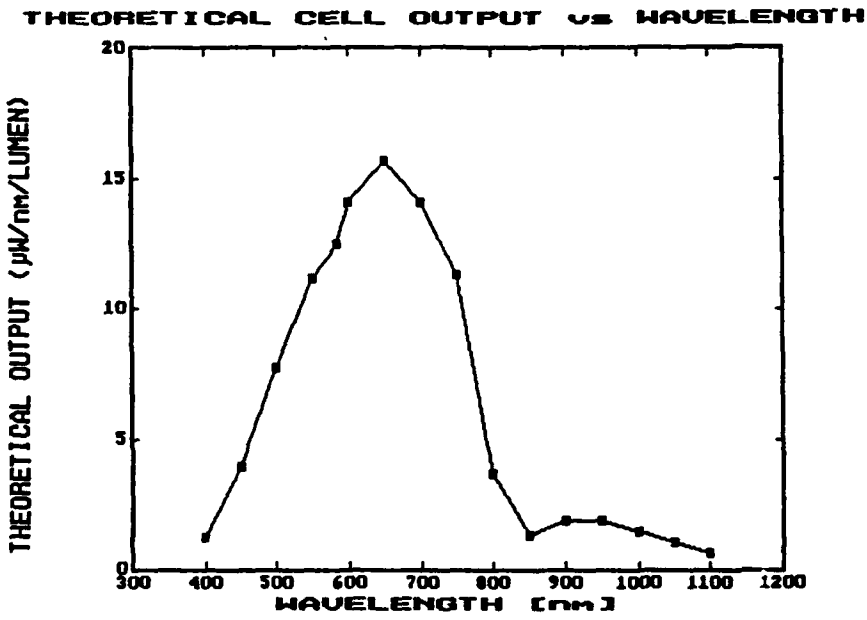

Graph 3. System performance of the halogen lamp and solar cell as a function of wavelength. This graph plots the product of the data shown in Graphs 1 and 2. It is the curve that would result if the hologram were 100% efficient at every wavelength.

Graph 4 is a typical output curve for one of the holograms. The output unit is the current recorded by the ammeter. If the hologram were 100% efficient everywhere, the curve would be identical in shape with the one shown in Graph 3, the only difference being a scale factor. To determine the appropriate scale factor, the diffraction efficiency of this hologram was measured independently at a specific wavelength (488nm).

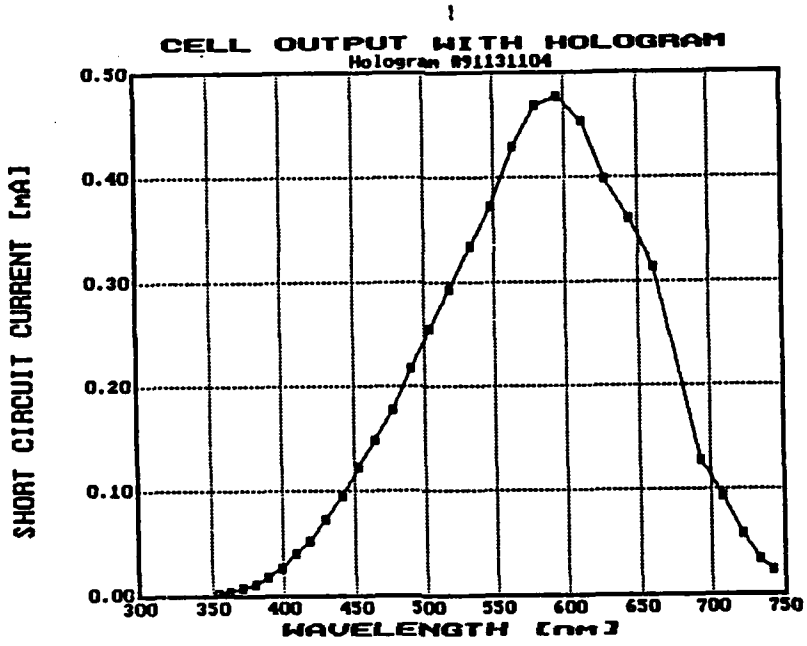

Graph 4. Output curve of the system with a typical hologram installed.

The diffraction efficiency of the hologram was determined at the argon wavelength of 488 nm. It is to be noted that all curves have a data point taken at 488nm and another at 633nm to aid in calibrating the curve at the argon and HeNe wavelengths. The efficiency η at 488nm was calculated, using Equation (2), by measuring the intensities D and U of the diffracted beam and the undiffracted beam, respectively.

$$\eta = D/(D+U) \qquad \text{Eq. (2)}$$

The diffraction efficiency of the hologram does not take

into account Fresnel reflection, which can be reduced or eliminated entirely by using antireflection coatings. For this particular hologram (#91131104) the efficiency at 488nm was found to be 87%.

Graph 5 shows the curve of hologram #91131104 together with the theoretical efficiency curve, adjusted so that at 488nm the efficiency of hologram #91131104 is 87%. If the hologram were 100% efficient these two curves would be identical. It is apparent that the efficiency of this hologram in this playback orientation (90°) is highest in the blue-green region of the spectrum and falls off in both directions. At the HeNe reference point of 633nm the efficiency is about 65%, which is consistent with the actual measurement made with a HeNe laser. All further curves use this standardized theoretical curve.

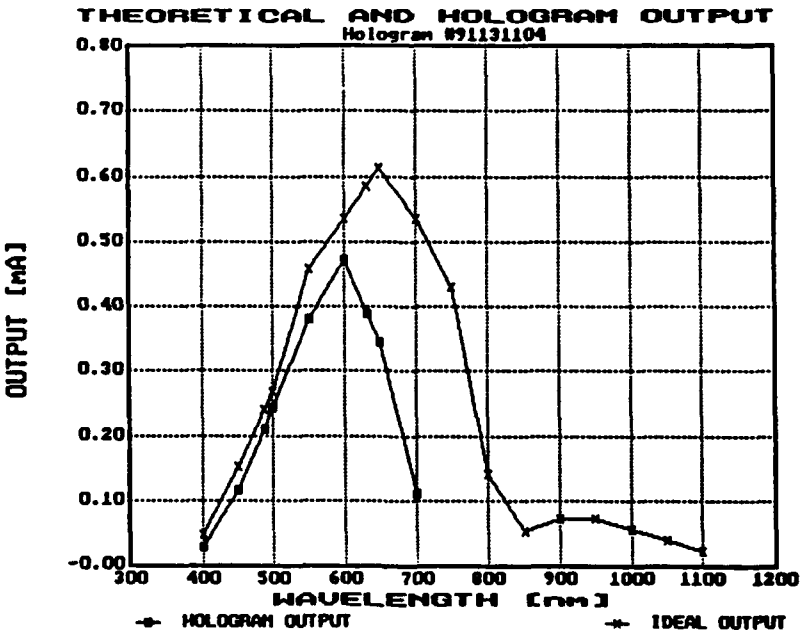

Graph 5. Hologram #91131104 and the theoretical output curve. The output curve has been normalized so that it is consistent with the 87% efficiency of the hologram at 488nm.

Graph 6 shows the efficiency of hologram #91131104.

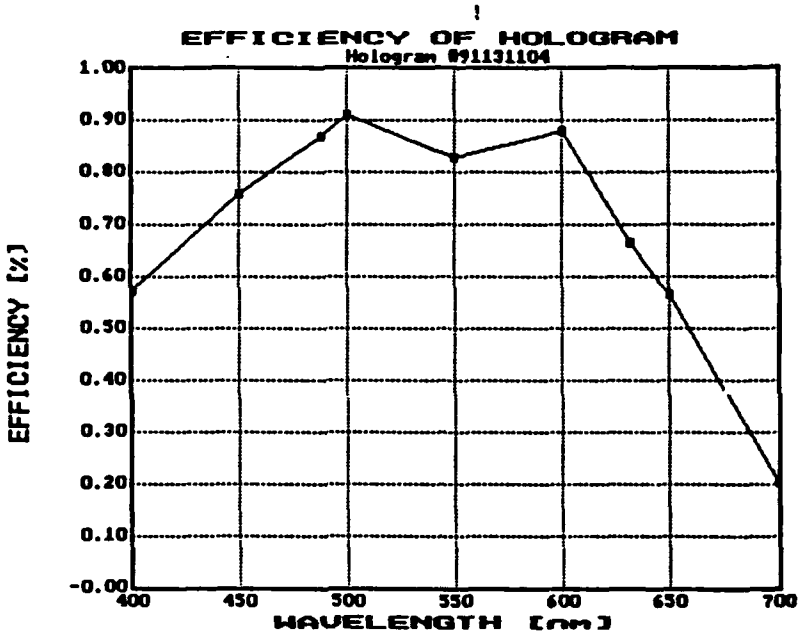

Graph 6. Absolute efficiency of hologram #91131104 as a function of wavelength. The hologram is at 90° to the incoming radiation. This hologram is 6 microns thick and has a calculated bandwidth at the half-power point of +/- 200nm.

Graph 7 shows the same hologram as Graph 6, oriented at 97° rather than 90°. The new orientation is optimum for the red portion of the spectrum. While in this orientation the efficiency at 488nm has dropped to 26%, the diffracted energy extends well into the red and infrared region of the spectrum, with an efficiency of 88% at 633nm. Since the hologram has, of course, the same thickness, the bandwidth is the same, +/- 200nm to the half-power points.

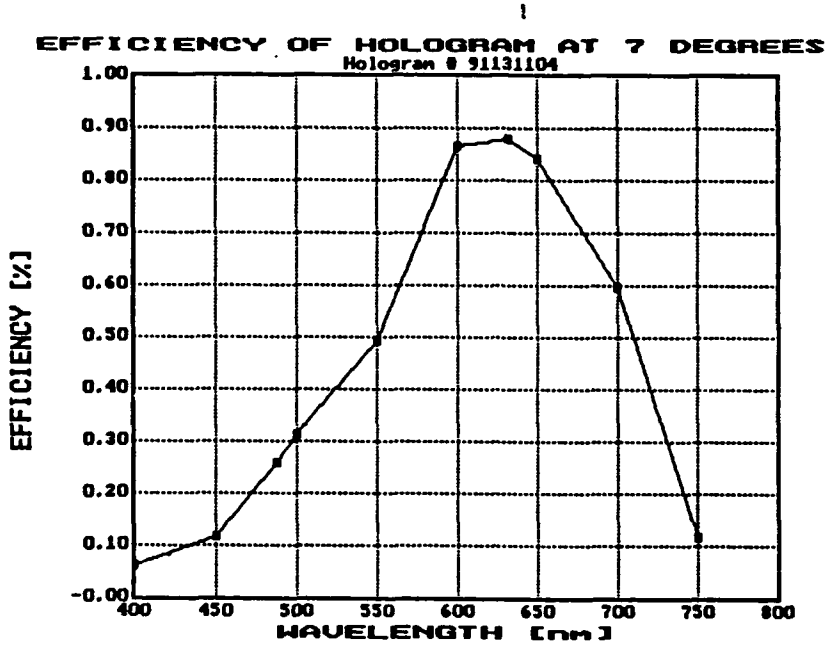

Graph 7. Efficiency of hologram #91131104 tilted to an angle (97°) such that the efficiency is a maximum at 633nm.

Depending upon orientation, this hologram can be highly efficient from the ultraviolet well into the infrared region of the spectrum. Thinner holograms will have a far more extended bandwidth for an orientation and structure optimized for the yellow-red portion of the spectrum, showing only moderate drop-off in the violet and near infrared regions. Graphs 8 and 9 show the efficiency of another hologram (#91101106) at 90° and 97°, respectively.

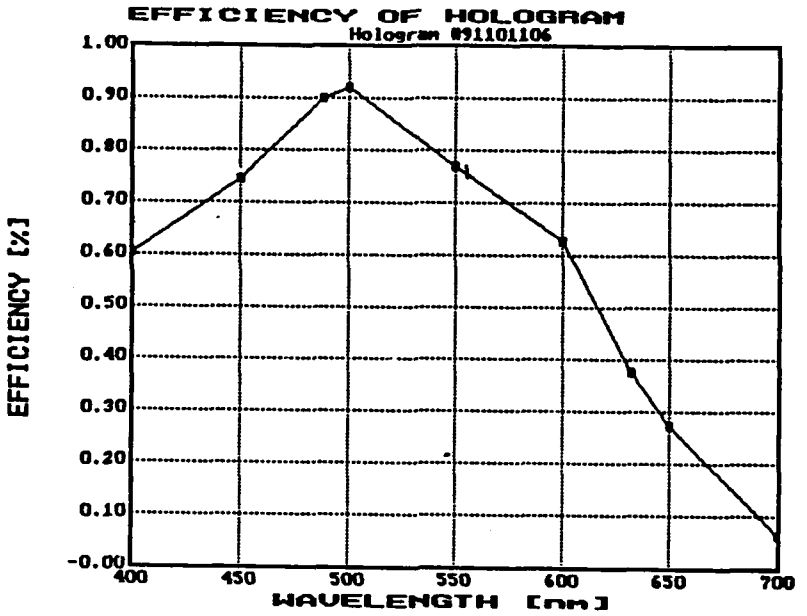

Graph 8. Efficiency of hologram #911011064 as a function of wavelength at 90° to the incoming radiation.

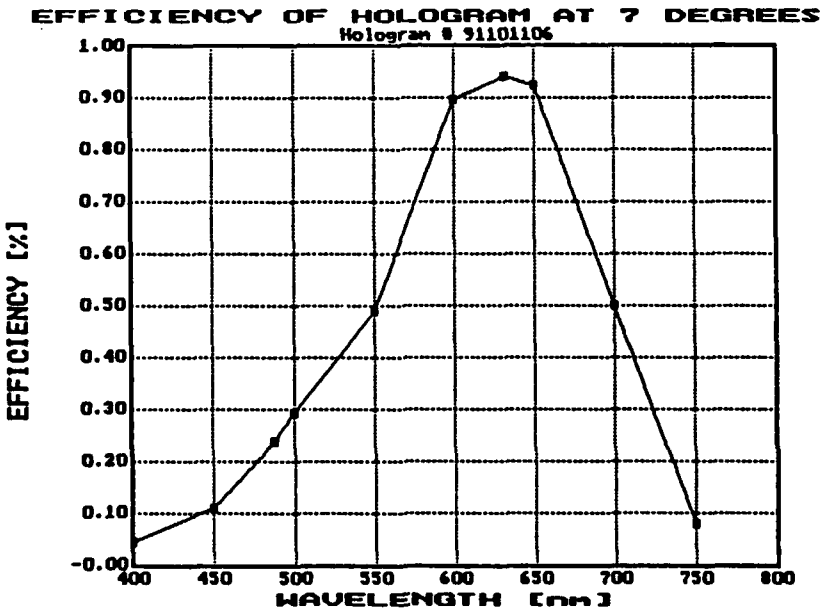

Graph 9. Efficiency of hologram #911011064 as a function of wavelength at 97° to the incoming radiation.

Efficiency tests were conducted on eight other holograms. Each hologram was first illuminated with an argon ion laser at 488nm (blue) and also with a HeNe laser at 633nm (red). The hologram was first oriented normal to an expanded beam from the argon ion laser. The diffracted light was focused by the hologram to an off-axis point, while the undiffracted light continued beyond the hologram and was focused by a lens to an on-axis point, as shown in Fig 4.

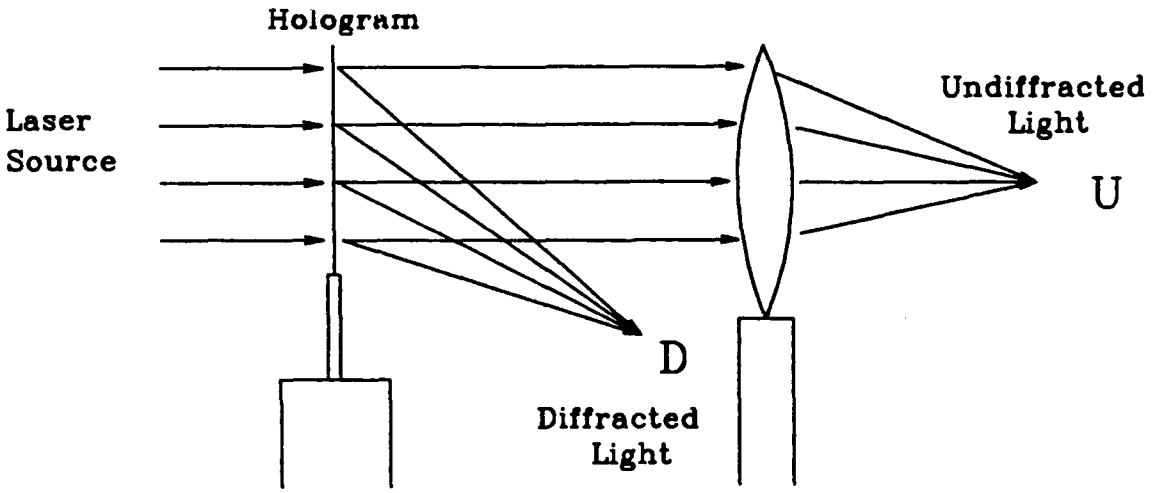

Fig 4. Testing the diffraction efficiency of a hologram. Intensities are measured at points D (diffracted light) and U (undiffracted light), and the efficiency calculated using Eq. (2).

The intensities of the diffracted and undiffracted light were measured with a power meter, and the efficiency $\eta_\perp$ calculated using Eq. (2). The hologram was then tilted until the diffracted intensity reached a maximum value, where the Bragg angle of the fringes was optimum for the incident wavelength. The angle θ_M and the efficiency η_M at that angle were measured. Tilting the hologram away from θ_M in either direction results in lower diffracted power. Measurements were made of the angles to which the hologram had to be tilted to reduce the diffracted power to half of its maximum value, and these angles (the half-power angles) were recorded. The entire process was then repeated using a HeNe laser.

If the hologram is tilted toward the laser source, the inclination of the fringes to the source changes and the efficiency curve shifts toward the red end of the spectrum, increasing the efficiency at 633nm and decreasing it at 488nm. To measure the efficiency for red radiation at the optimum angle for blue light, an additional set of readings was taken, using HeNe radiation but with the hologram tilted at its optimum angle for argon radiation. Then the argon ion laser was again used and a further set of readings made, this time at the optimum angle for the red HeNe wavelength. In Table II, in rows for 488 nm, the efficiency for 488nm radiation at normal incidence is shown in the column labeled "$\eta_\perp$", its optimum angle in column "θ_M", and its maximum efficiency in column "η_M". The efficiency at that same angle for light of wavelength 633nm is listed under the heading η^*_M. The half-power angles are in columns "$\theta^+_{½}$" and

"$\theta^-_{½}$". In rows for 633nm, of course, the wavelength values are interchanged.

TABLE II

Efficiencies, Optimum Angles, and Half-power Angles for Several Holograms at Two Wavelengths

Hologram #	nm	$\eta_\perp$	θ_M	η_M	η^*_M	$\theta^+_{½}$	$\theta^-_{½}$
91102502	488	89%	90°	89%	68%	96.5°	83.5°
	633	63%	95°	93%	63%	89.5°	114°
91131104	488	87%	90°	87%	57%	97°	84°
	633	55%	96°	88%	55%	103°	90°
91101102	488	73%	90°	73%	59%	98°	84°
	633	50%	96°	70%	50%	105°	88°
91101106	488	90%	90°	90%	48%	98°	86°
	633	39%	98°	94%	39%	103°	91°
91102501	488	60%	90°	70%	52%	97°	86°
	633	29%	97°	82%	29%	103°	92°
91110402	488	63%	90°	63%	56%	99°	85°
	633	20%	97°	76%	20%	104°	92°
91102505	488	66%	90°	66%	40%	96°	84.5°
	633	44%	96°	67%	44%	102.5°	89°
91101105	488	56%	92°	69%	24%	96°	89°
	633	7%	98°	86%	16%	102°	95°

HARDNESS OF MATERIALS TO THE SPACE ENVIRONMENT

These holographic solar power concentration and spectral separation systems must be able to operate in the environment of space, which is characterized by a vacuum of 10^{-8} to 10^{-9} torr in the presence of charged particles and electromagnetic radiation. The effects of the environment on the holographic material, the substrate material, the solar cells, and the support structure must be taken into account and may affect the choice of materials. The effects that must be considered are those of high vacuum, charged particles, electromagnetic radiation, ultraviolet in particular, and, during the time period prior to launch, humidity.

The first area of interest is the space hardness of the holographic materials and their substrates. There are several possible holographic materials of choice, including dichromated gelatin, the Polaroid photopolymer, and others. The material used for preliminary testing and demonstrations of feasibility in this Phase I effort was dichromated gelatin on glass. The effects of the space conditions on dichromated gelatin have been extensively studied.[8] The major effect of the high vacuum of space is the loss of 3% to 4% of weight, due primarily to the evaporation of water. This results in a small change in the spacing of the Bragg planes, which leads to a shift of the location where each wavelength focuses. The change in spacing could be compensated by calculating it before launch and locating the solar cells in positions for the new spacings. However, since experiments[8] on holographic filters have shown a change

of only about 30nm in peak wavelength and our solar cells are broad-band, such compensation is probably unnecessary. The holograms can be protected against changes in humidity by sealing them under a protective cover glass or plastic, using acrylate adhesive and low-outgassing epoxy. The adhesive or epoxy is used to cover the entire surface of the hologram as well as the edges, so that the seal is everywhere. Degradation of the protective color at a particular location, for example by a micrometeorite, affects only that specific location, not the entire unit. This procedure minimizes the effect of vacuum on the holograms, as well as the effects of pre-launch humidity changes. Fig 5 shows a cross-section of a hologram sealed by this technique.

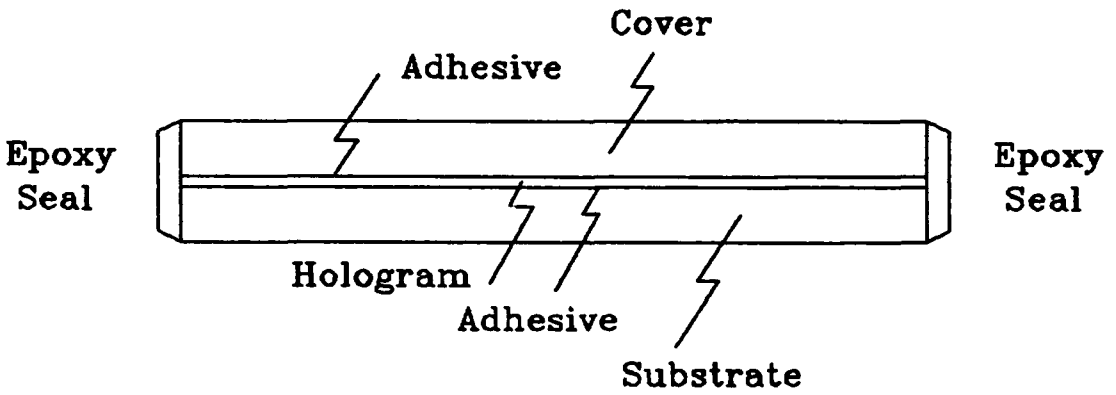

Fig 5. Method of sealing holograms against the effects of humidity.

The effects of charged particles and of electromagnetic radiation on the dichromated gelatin are minor.[8] Simulated exposure to five years of the proton flux of space resulted in only minor shifts in the wavelength characteristics of

holographic filters and a moderate decrease in light transmission below 500nm. Holograms exposed to a source of ultraviolet radiation equivalent to 16 suns for 69 days (1104 days equivalent solar exposure) resulted in no decomposition of the structure of the dichromated gelatin.

The Polaroid photopolymer DMP-128 is a candidate for use in this program because of a number of favorable features. It can be fabricated in thin films that are highly efficient, permitting very broad bandwidth operation. The material is also intrinsically much less susceptible to moisture than is dichromated gelatin. Measurements made on the Polaroid material to determine the resistance to ionizing radiation[9] of holograms on that material have shown a remarkable degree of hardness. The study used medium thickness holograms on radiation-resistant glass plates (CFQT-20 Suprasil). The devices tested were of relatively low efficiency, but that efficiency showed negligible change, as did both the amount of light diffracted and the direction in which it was diffracted, after exposure to 2 Mrad (Si) 63 MeV protons and also after Co60 gamma ray doses of 2 Mrad (Si). Since these radiation levels can be expected to disrupt the structure of a polymer and since the effectiveness of materials exposed at this level might well be degraded in other ways, it appears clear that the holographic information stored is essentially not a function of the amount of polymerization.

The holographic process in this material and most others appears to be one in which, after the process is completed, the

amount of cross-linking in one region or another is followed by a structure in which the index variation, the density variation, and the density of microvoids, fissures, cracks, and the like are common. Later breaking of cross-linked bonds will not affect this structure and will leave the hologram as a functional element. The hologram, then, is essentially more radiation resistant than the material from which it is made. This consideration, of course, does not apply to moisture or vacuum effects that would directly alter the structure of the material rather than its internal bonding structure. Even in the Van Allen belt, doses of the order of 1 Mrad/year are typical. These materials do not present a significant problem for typical satellite operation.

The effects of the space environment on various possible holographic substrate materials and structural materials has also been reported in great detail[10]. The generally accepted criterion for exposed structures is exposure to 10^9 rad without significant degradation.

There are a number of other requirements besides radiation resistance that are important for some of the materials. Non-volatility is a stringent requirement for adhesives and sealants, since these materials are applied as liquids, so care must be taken to eliminate all volatile substances during their preparation. This can often be achieved by complete curing or by heating in a vacuum to remove residual solvents and monomers.[10] Special care must be taken to balance this heating requirement with potential damage to the structure of the holographic

material itself when one is preparing a suitable protective bonding structure for this application. The properties of some of these sealants and adhesives are often sensitive to temperature, so their behavior at temperature extremes is essential to selecting the appropriate material.

The environments encountered in space vary widely, depending upon the altitude and orbit of the spacecraft.[10] Earth-orbiting spacecraft at high altitudes encounter trapped electrons and protons where the doses to the exposed surfaces may exceed 10^7 rad/day. Since this dosage affects only the top micron of the material it is not important, except where it may affect the optical properties of the material protecting the hologram. If the hologram itself were exposed, these dose levels would be very important. For lower orbiting spacecraft the radiation is less, except for those in orbits over the poles or over the South Atlantic anomaly.

Some of the candidate materials, such as Mylar, PET, and PBT are polyesters that have appropriate spectral properties both for substrate material and for protective covers if glass substrates are used. Their optical problems are a relatively high birefringence, which is not a serious problem in the geometry that we are using. They have excellent radiation resistance. The filled structures, with either glass or mineral filling, exceed 10^9 rad. The radiation resistance of the unfilled structures is greater than 10^6 rad. Even this lower radiation resistance is sufficient to allow operation for periods of a few

years. Higher dosages occur only in the material's skin. Some candidate materials, such as the fluorocarbons (Teflon), are not suitable for this application because of degradation of their properties, as well as the release of potentially corrosive by-products. Our observation of Teflon under gamma radiation from a Co60 source confirms that its structural integrity is destroyed.

It can be concluded that care must be taken in the choice of materials for space applications, but that there are ample candidate materials that have long life with high stability in a space environment for structural, substrate, and protective covering applications.

SOLAR CELL TECHNOLOGY

The generation of power using solar radiation and solar cells can be accomplished in a number of ways. The simplest but lowest efficiency technique is to use flat panels and incident radiation directly. A better technique is to use the same systems but with solar tracking, which in the case of space power generation is not an additional requirement since the tracking capability is a feature of orbiting satellites. Substantial additional improvement can be obtained by focusing and concentrating the radiation, as will be described in the following. A still further improvement is possible using two or more solar cells with different characteristics if the solar spectrum is appropriately split to deliver the appropriate portion of the spectrum to the corresponding cells. The fundamental reason for the advantage of the multiple cells is that a given cell has a characteristic energy bandgap which corresponds to a particular wavelength of incident radiation.

The combined effect of photon energy in excess of the bandgap and photons with energy less than that required to generate charge carriers results in energy losses in solar cells. These losses amount to more than half of the energy absorbed by a conventional solar cell. If the bandgap energy of the cell is increased, the first contribution is decreased, but the second will rise. Clearly, these losses could be made much smaller if the light incident on a given cell were matched to the bandgap energy. (1)

Two traditional arrangements have been proposed to take advantage of this fact. The tandem or cascade cells have cells with different bandgap energies superimposed upon each other in such a way that the lower cells utilize progressively longer wavelengths. The spectrum splitting arrangement uses special filters to separate the incoming

light into bands of different wavelengths so that each band can be directed to a matched cell. The tandem cell scheme does not require the filters or mirrors but places more stringent requirements on the minimization of spurious absorption and reflection in each cell and of shadowing by the front and back contacts.

We have proposed that thick holograms constitute an advantageous alternative to the filters and mirrors but primarily because the holographic spectral splitting is far more efficient. The transmission efficiency for holograms is extremely high, on the order of 90 to 95 percent. Furthermore, the holograms combine the effects of spectral splitting with concentration, thus minimizing structures and costs for these systems. Much of the work previously performed for systems based on filters or tandem cells can be used to scope the potential for the holographically-enhanced photovoltaic cells.

In particular, we may draw from the analysis of a two-cell system made by Masden and Backus (11). The results are summarized in Figure A, where the calculated efficiency at a concentration of 100 times is plotted as a function of the bandgap energies of two cells for terrestrial applications (AM2). The graph shows that a peak efficiency of 42 percent can be achieved with the combination of two cells whose bandgap energies are, optimally, 0.95 eV and 1.75 eV.

The graph also highlights some promising near-term cell candidates. If one is interested in taking advantage of inexpensive, readily available Si cells, both the GaAs/Si system and the Si/Ge system yield an efficiency of about 34%. On the other hand, a GaAs/Ge system can achieve efficiencies as high as 37%: the large difference between the bandgaps of GaAs and Ge allows these two cells to cover the solar spectrum to advantage. It may be argued that since

absorption in the atmosphere is particularly effective at very short and very long wavelengths; i.e., since the differences between the AM2 and AM0 spectra are particularly high at the tails of the spectra, as shown in Fig. B. reproduced from (13), the GaAs/Ge system is likely to be an attractive one in space. (Our group is working at reproducing this analysis for AM0 conditions).

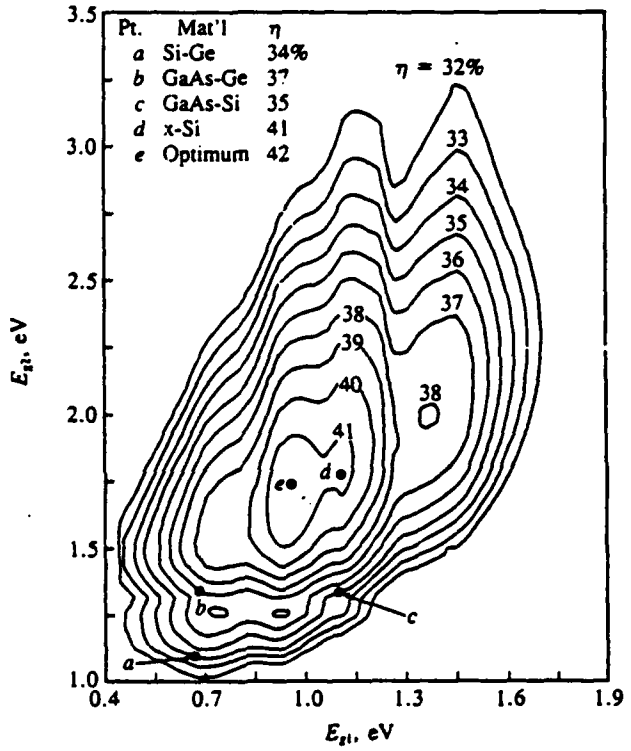

Fig. A

Limit conversion efficiency contours for two-cell spectrum-splitting systems for AM2 and 100× concentration. (*Masden, 1978.*)

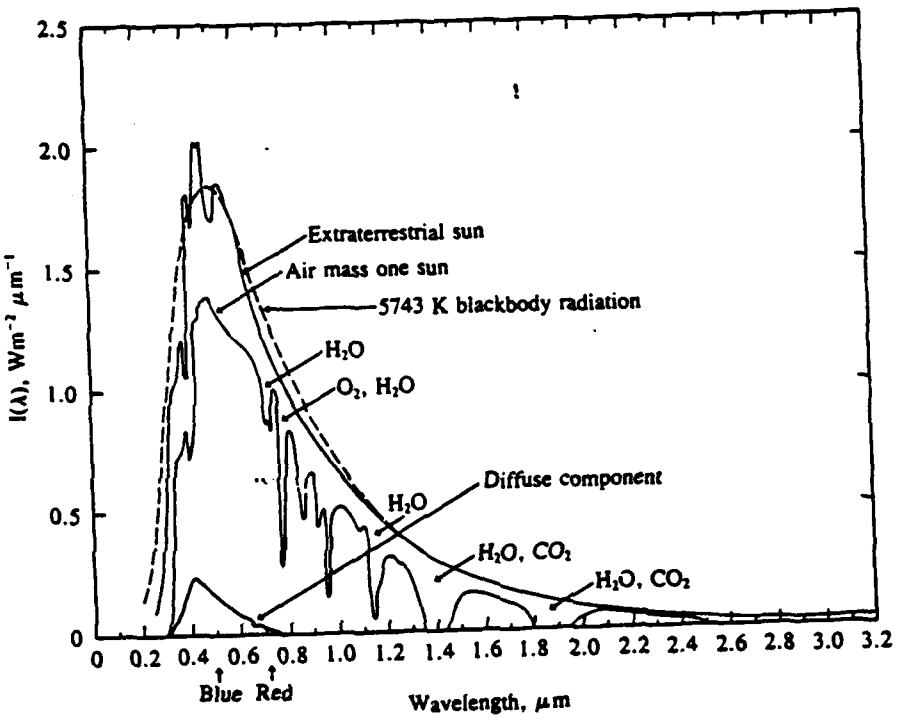

Spectral intensities of the extraterrestrial and air mass one (sun directly overhead, measured at sea level) direct solar radiation. A typical spectrum of clear sky scattered radiation is also shown.

Fig. B

The choice of which of these options is best will depend on many factors. One is the environment under which the system is to be operated. Notably, the choice will depend on the expected operating temperature of the system: Masden's graph does not give an indication of what concentration-induced heating can do to these values for efficiency.

TEMPERATURE EFFECTS

The efficiency of a given cell under illumination from sunlight can be written as the product of the open circuit voltage times the short circuit current times the fill factor of the cell divided by the incident solar power.

The open circuit voltage can be written as:

V_{oc} = (energy gap/charge) - (kt/q) times (a logarithmic term)

The second term in this equation is basically constant, and it is typically 0.5 volts. Thus, the open circuit voltage increases with increasing band gap, Eg. Si , with an energy gap of 1.12 eV, has an open circuit voltage of about 0.5 volts; GaAs, with an energy gap of 1.43 eV, has an open circuit voltage of about 0.9 volts.

On the other hand, the maximum possible short circuit current decreases with increasing Eg. As a result, the upper limits of solar conversion efficiency for a cell peak at a certain Eg. This is illustrated in Fig. C, where the calculated upper limit of efficiency is plotted for unit collection efficiency, at a doping concentration of 10^{17} cm^{-3} and typical lifetimes. Clearly these maxima can be exceeded in systems where several solar cell materials are employed. What is of interest here is the effect of temperature on efficiency.

Figure C. shows that the efficiency decreases with increasing temperature. Since the short circuit current is insensitive to the temperature, it is the open circuit voltage that is responsible for much of the temperature dependence of the efficiency.

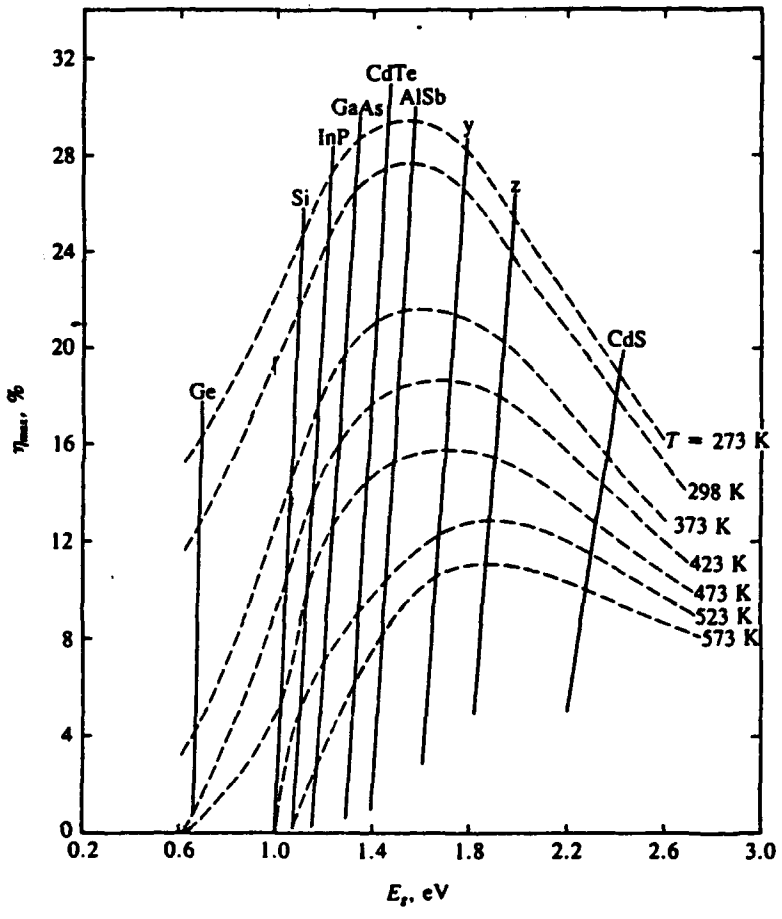

Fig. C. Calculated upper limits of efficiency. Assumptions: Unity collection efficiency, 10^{17} cm^{-3} doping, typical lifetimes. These limits may be exceeded by using light concentration or employing more than one solar cell material. *(Rappaport, 1959.)*

From the equation for the open circuit voltage,

$$dV_{oc}/dT = (1/q)(dE_g/dT) - (k/qV) \text{ times (a logarithmic term)}$$

$$= (1/q)(dE_g/dT) - (1/T)(E_g/q - V_{oc})$$

For Si , $dE_g/dT = -0.0003$ eV/C, $E_g/q - V_{oc} = 0.5$ V, and therefore $dV_{oc}/dT = -2$ mV/C. Thus, for every 1 C increase in temperature, V_{oc} drops by about 0.002/0.55 or 0.4% of its room temperature value, and hence the efficiency drops by about

the same percentage. For example, a Si cell having 20% efficiency at 20 C will only be about 12 % efficient at 120 C.

For GaAs, V_{oc} drops by 1.7 mV or 0.2 % per C. If the term $(1/q)(dE_g/dT)$, can be neglected in the last equation, dV/dt can then be predicted if one knows the energy gap and the open circuit voltage of any given cell (1).

The efficiency achievable from a cell decreases as the cell is heated, and the decrease is more pronounced for a low-energy gap cell. Since the figure from Masden was drawn for a system at a concentration of 100 times, it is useful to consider the effect of concentration on the temperature of the cell.

Before considering the effect of concentration, it is useful to write down the expression for the total effect of temperature T on the efficiency h of a cell:

$$dh/dt = (1/P_{in})[I_{sc}V_{oc}(dFF/dT) + Isc\ FF\ (dV_{oc}/dT) + V_{oc}FF\ (dI_{sc}/dT]$$

In this equation, FF is the fill factor. The Voc, FF, and Isc temperature coefficients for a given cell, such as silicon, are different when used singly or when used in a multijunction cell. It will be noted below that this has important consequences for the performance of the stacked cell.

OBSERVATIONS ON MECHANICALLY STACKED, MULTIJUNCTION SOLAR CONCENTRATOR CELLS

A short discussion of the thermal behavior of the "traditional" mechanically stacked, multijunction solar

concentrator (MSMJ) cells will help to highlight some of the advantages of the concept advanced here.

The normal operating cell temperature of mechanically stacked cells in a concentrator module is higher than that of a single-junction cell. This is due to the stacked cell construction itself. This reduces, or may even negate, the expected performance advantages of MSMJ configurations in a concentrating system. This has been well documented for GaAs-based cell (13).

In a MSMJ cell, the bond between the top component cell and the bottom component cell must serve several functions, such as mechanical adhesion, electrical isolation, optical coupling, and thermal conduction between the cells. Not surprisingly, the requirements for some of these functions conflict.

In a typical "vertical" MSMJ assembly, the top cell is bonded to the bottom cell with an adhesive layer, and heat generated in the top cell must be conducted vertically through the cell assembly to the heat sink. Silicone adhesives and glasses are candidate materials: silicone has poor thermal conductivity, but glasses require higher temperature processing, and this higher temperature may damage the cells. If silicon is used, the largest temperature drop in the stack is that across the adhesive layer: to minimize this drop, the adhesive layers be made very thin (less than 25 microns), and producing this thin bond reliably without shorting the top and bottom cells may be a concern.

In any case, if the temperature of the bottom cell is determined by that of some heat sink, The top cell (the GaAs cell, for example) is at a higher temperature than it would be in a simple junction cell, and any advantage associated

with the bottom cell is offset by the decrease in performance due to the negative thermal coefficient of the efficiency of the top cell.

To ameliorate these concerns, a horizontal assembly may be considered. (14) In this configuration, the cells are mounted centered over a hole on either side of a heat spreader, made up, for example, of two layers of copper separated by a dielectric. In this configuration, the heat generated in each cell is conducted horizontally across the cell to the heat spreader. This imposes limits on how large the cells can be, and on how large the fraction of the surface area of a module can be made up of cells. Another disadvantages of this arrangement is that the bottom cell operates at a higher temperature than in the vertical stack. In the stacked arrangement, the low energy gap cell would be the bottom cell, and the performance of low energy gap cells such as germanium is more affected by temperature than GaAs. Also, because the temperature profile across the cell is very dependent on the illumination of the cell, the performance is very sensitive to the flux profile. Finally, it is clear than the horizontal assembly places severe constraints in the cell size.

The challenge induced by the thermal dissipation in stacked cells can be even more constraining in the case of more complex arrangements such as mechanically stacked two-tandem concentrator solar cells (15).

One effect which tends to improve the performance of a vertically stacked multijunction cell is, interestingly, the temperature coefficient of the short circuit current on the low-energy gap cell. Consider, for example, the effect of stacking on a silicon cell which may serve as the bottom cell. The short-circuit current on the stacked silicon cell is much lower (by a factor of, say, 7) than it would be if

used as a single- junction cell. Since the short-circuit current affects the temperature coefficient, the temperature coefficient of the Si cell is better when it is used as the bottom cell in a stack. Note that this effect, which helps the multijunction cell, would be also present in a holographically enhanced cell, where the spectrum is split before it reaches the cells.

In most discussions on the performance of MSMJ cells, the assumption is made that either the bottom cell or both cells are somehow in thermal contact with a heat sink. This assumption is convenient, but the design of the sink may itself be a problem in space if much thermal energy must be removed. This would certainly be the case of concentrating systems which are expected to generate a lot of power. This is discussed next.

THE EFFECT OF CONCENTRATION ON CELL TEMPERATURE

Sunlight can be focused or concentrated so that the same amount of electric power can be produced from a smaller cell area. If the incident sunlight is concentrated by a factor of C>1, both the input power per cell area and the short circuit current are multiplied by C. The open circuit voltage, however, increases by (kT/q) ln C, that is, 0.12 volts for a concentration of 100. *The output power, therefore, increases more than C times. Thus, concentration increases the conversion efficiency as long as the cell is maintained at a constant temperature.*

On the other hand, it is obvious that concentrated radiation will also raise the total heat energy deposited or dissipated in the cell. Unless measures are taken to cool the cell, it will be heated. Since this lowers the conversion efficiency of incident sunlight to electricity,

the extra heat deposition will be multiplied by a factor higher than the concentration, C. This makes it particularly important to minimize those losses associated with insufficient or excessive photon energy, since the unusable photon energy is converted to thermal energy. In other words, splitting the solar spectrum may be particularly important for concentrating systems.

On earth, it is always possible, in principle, to cool a concentrating system, although the cooling solution may affect the costs and the reliability of the system. While it would appear that cooling should be no problem in deep space, the design constraints may be more limiting if cooling is needed.

Assume that we have a solar converter in space, so that the solar irradiance on the converter is q (W/m2). Further, to maximize the efficiency of the converter, assume that it is designed so that it reflects none of the radiation incident upon it. In the absence of cooling fins, one may estimate the temperature which the surface will attain by assuming that it is cooled by radiative cooling in space at effectively zero temperature (16). At equilibrium, the absorbed energy, which is equal to the product of the absorptance, α, times q, must be equal to the radiated energy, which is equal to the Boltzman constant σ times the emittance, ε, times the fourth power of the absolute temperature, T.

Solving for T,

$$T = (\alpha q/\sigma\varepsilon)^{1/4}$$

Using for q the solar constant at a position in space approximately equal to that of the earth, we have

$$T = (\alpha q/\sigma\varepsilon)^{1/4} = 393 \text{ K} = 120 \text{ C}.$$

A Si cell having 20% efficiency at 20 C will only be about 12 % efficient at 120 C. Of course, this calculation assumed that none of the incident radiation was converted to electricity, or that the electricity eventually was dissipated as heat and remained in the cell. If one had assumed that somehow the cell had a fixed 12% efficiency, then T = 96 C. If neither of these assumption is valid, an iterative procedure must be followed to estimate the equilibrium temperature of the cell. However, overheating does not seem to be much of a problem.

Cooling *is* a problem for a traditional type of concentrating system. For example, using again the solar constant for a system orbiting the earth, even for a concentration as low a 10, a "black" surface would be at equilibrium at T = 698 K, at which temperature a Si cell could not operate.

Even for a concentration as low as 4, under the same assumptions, the equilibrum temperature would be about 555 K, at this temperature, no useful power would be drawn from a Si cell.

It is obvious that the challenge is much alleviated in the case of a scheme in which the spectrum is split, although the calculations can be considerably more difficult. Difficulties arise partly because the concept of concentration itself is not well defined in the case where different parts of the spectrum are aimed at different converters.

Holographic Enhancement of a Simple Si Cell.

Consider the straightforward case in which holograms are used to enhance the performance of simple Si cells. The energy gap for Si is about 1.12 . (The energy gap itself is not a strong function of temperature for Si). This corresponds to photons of about 1.098 microns. A fraction of about 0.257 of the solar radiation at AM0 is at wavelengths higher than this. A configuration in which photons with wavelengths greater than about 1.1. "miss" the silicon cells will increase the efficiency of conversion of the intercepted flux in two ways.

• First, the configuration will increase the efficiency with which the intercepted sunlight is converted to electricity, since photons of insufficient energy are diverted elsewhere. In terms of the total sunlight intercepted by the collector (in this case the hologram), this clearly does not directly add to the electrical output. However, in terms of the power generated per unit area of the cell, this automatically reduces the losses by a factor of about 25%.

• Second, if there is no "hit" there is no "heat". Those useless low energy photons are not adding to the heat load on the cell, which is thus decreased by a factor of 25%. This lowers the equilibrium temperature of a black surface at any concentration by about 7%. Thus, for a four-fold concentration of the number of photons with energies above the silicon gap, the absolute temperature of a blackbody would be now 516 K. This simple consideration implies that the cell can now operate.

The heating and the losses could be further reduced for a simple Si cell by deflecting the very high-energy photons. Suppose, for example, that photons with wavelengths less than 0.868 microns were to miss the Si cell. (This corresponds roughly to the energy gap of GaAs). Since these photons make

up about 60.7% of the solar spectrum, now only about 14.3% of the sunlight reaches the Si cells - but this 14.3% is the "good part" of the spectrum for silicon. Now the absolute temperature of the blackbody at a "concentration of 4" would be only about 341 K, i.e., more than 51 K less than the non-enhanced cell with no concentration.

The net benefit of the simple configuration is more than the sum of these two effects. The increased efficiency at lower temperature means that since more of the intercepted power is converted to electricity, there is less dissipated heat. And, clearly, our proposal is that those energetic photons be holographically redirected to a cell with a higher energy gap.

HOLOGRAPHICALLY ENHANCED MATCHED CELLS

Consider now a photovoltaic system with Si and GaAs cells. Suppose that the spectrum is now roughly divided into three bands, one with photons of wavelengths greater than 1.098, one with photons of wavelengths between 1.0987 and 0.868, and the last one for photons with shorter wavelengths. The first part comprises 25% of the spectrum, and is aimed so that it does not hit any cells. The second part comprises about 13.5 % of the spectrum, and is aimed at the Si cells. The last band, comprising about 60.7% of the spectrum, is aimed at the GaAs cells, which can tolerate relatively high temperatures.

By practically eliminating the "energy mismatch" on the Si cells, they can now operate at a relatively low temperature even in a concentrating system. Thus, the silicon cell could convert to electricity close to about 10% of the total incoming solar spectrum. There would be no losses because of low-energy mismatch in the GaAs system, which serves 60.7 of the spectrum. Thus, it would be possible to achieve overall efficiencies of close to 40%.

DISCUSSION

It has been demonstrated that holographically enhanced systems have the potential for improving the performance or photovoltaic systems for space applications and that the resulting systems would be of light weight.

In traditional multijunction solar concentrator cells, the "top component cell" must be bonded to the bottom component cell, and the bond must serve several functions which often impose conflicting requirements. Further, at high concentration, even if the cells have access to an effective heat sink, thermal gradients within the cell will affect the system performance Thus, materials which would be attractive candidates to work in multijunction cells because their energy gaps match the solar spectrum at AM0, may not be acceptable because of the conflicting requirements imposed upon the MSJM cell design.

Holographically enhanced photovoltaic systems have the potential to eliminate most of the problems encountered in traditional multijunction solar concentrator cells. The holograms themselves have very high efficiencies and can achieve high concentration when deflecting the desired photons onto the cells with matching energy gaps. Further, even at high concentration, cooling is not a problem because the cells are not stacked. The alleviation of the heat dissipation problem makes it possible to design much simpler and lighter systems. Also, since the cells are not stacked, they do not interfere with the performance of each other, and the problem of choosing the cells with the optimum gap can be solved without the many constraints imposed by other requirements in the stacked cell.

The holographically enhanced cells do share with the MSMJ the advantages of the latter, however. The most obvious one is that they allow a match of the different bands to different converters. More subtle advantages are clear under careful consideration.

The temperature coefficient for the efficiency of a cell depends on the effect of temperature on the fill factor, open circuit voltage, and shortcircuit current. It is well understood that, in an MSMJ system, a bottom "low energy gap cell", such as Si, has a better temperature coefficient than the same cell has when used singly. The reason for this is that when the silicon cell is operated under the filter of a high-energy cell, the short circuit current in silicon is much reduced. Because of this, the short circuit term becomes negative, and counteracts the effect of the fill factor and open voltage terms.

This positive effect also occurs with the holographically enhanced system, because the high energy photons do not illuminate the low energy cell and the short circuit current is reduced.

On the other hand, the effects which often make the performance of MSMJ system so disappointing do not affect the holographically-enhanced system.

For example, the energy bandgap of a GaAs cell decreases with temperature. In an MSMJ system, when the top cell heats up, there is less power generated in the GaAs cell, but there is also less light reaching the bottom cell.

One of the most attractive features of the holographically enhanced system is that it cleanly decouples the problems of spectrum-cell matching from other thermal or structural

challenges. This is true for systems composed of two cells or several.

In spite of the obvious attractiveness of the Ge/Si and Ge/GaAs systems, the group has decided to concentrate on the GaAs/Si cell for this project. We do not know a priori what the operating temperatures for the envisioned concentrating system are, but the efficiency of conversion for germanium is very low at high temperatures. The energy gaps for GaAs and Si are relatively close, and therefore a relatively smaller fraction of the spectrum is aimed at Si cell rather than at GaAs. However, Si cells operate less effectively at higher temperature than GaAs, and so this arrangement is justified.

References

1. Hu, C., and White, R. M., Solar Cells: From Basic to Advanced Systems, McGraw Hill Book Companyh, New York, (1988), pp. 238-241.

2. Saxby, G., Practical Holography, Prentice Hall, New York (1988), pp. 276-278.

3. McGrew, S. T., SPIE Proc. 215, 27 (1980)

4. Kogelnick, H., Bell Systems Tech. J. 45, 2909, (1969)

5 Caulfield, H. J., Handbook of Optical Holography, Academic Press, New York (1979), pp. 385-387.

6. Ludman, J. E., Am. J. Phys., 50, 244 (1982)

7. National Technical Systems, Technical Report # 85-1501 (1985).

8. McKay, A. and White, J., SPIE Proc. 1044, 269 (1989).

9. Golden, J. P., Summers, G. P., Carter, W. H., Optics Letters 13, 949 (1988).

10. Frederickson, A. R., Cotts, D. B., Wall, J. A., Bouquet, F. D., Spacecraft Dielectric Material Properties and Spacecraft Charging, Am Inst. of Aeronautics and Astgronautics, New York (1986), pp. 40-50.

11. Masden, G. W., and Backus, C. E. , 13th IEEE Photovoltaic Spec. Conference Record, p. 853 (1978)

12. Duffie, J. A. and Beckman, W. A., Solar Engineering of Thermal Processes, Wiley, New York (1991)

13. Gee, J. M., and Chiang, C. J., The Potential Performance of GaAs-Based Mechanically Stacked, Multijunction Solar Concentrator Cells, Twenty First IEEE Photovoltaic Specialists Caonference - 1990, I, Kissimimee, Florida.

14. L. M. Fraas et al., Trans. Elect. Dev., **ED-37**, 443 (1990)

15. Beaumont, B., Leroux, M., Guillaume, PJ. C., Gibart, P., and Verie, C., in 6th EC-PSEC, Freiburg (1985), p. 521.
Not true in the hologram.

16. Martín, J. G., and Blanco, M., Radiation Heat Transfer, Handbook of Applied Heat Transfer, E. Guyer, ed., McGraw Hill (1989).